A methodology for radiometric calibration of remote sensing images

Alireza Sharifi[1] and Elaheh Moradi[2]

[1]Shahid Rajaee Teacher Training University, Civil engineering faculty, Tehran, Iran

Email: a_sharifi@srttu.edu

[2]Shahid Rajaee Teacher Training University, Civil engineering faculty, Tehran, Iran

Email: elahemoradi93@gmail.com

ABSTRACT: One of the most important calibration in remote sensing is sensor radiometric calibration that means computing physical values of radiance of the investigated targets. Radiometric calibration usually relies on pre-flight and vicarious calibration or on indirect approaches. This paper introduces an experimental approach that makes use of on-board calibration techniques to perform the radiometric calibration of the Landsat 8 data. This approach relies on the use of a calibration methodology which developed to convert the raw output from the instrument into an accurate at-aperture radiance. The radiometric accuracy was estimated to be approximately 1.4%. The calibration parameters were updated during the post-launch checkout penod by using ground targets. In addition, the absolute calibration performance determined from vicarious measurements have revealed a time-varying error to the absolute radiance. Analysis of results seems to point out limitations of traditional radiometric calibration methodology based only on pre-flight approaches, with important implications for data quality assessment.

KEY WORDS: radiometric calibration, remote sensing, WorldView-2.

1. INTRODUCTION

To enable quantitative information to be obtained from multispectral satellite sensors such as WorldView-2 factors affecting the raw digital numbers (DN) such as sensor characteristics, radiometric effects need to be removed (Smith & Milton 1999). A number of different methods have been developed to correct these effects on satellite imagery. These include image based methods (Chavez 1996), radiative transfer models (Vicente-Serrano et al. 2008) and the empirical line method (Smith & Milton 1999).

The purpose of the study is to assess the ability of the empirical line method to convert multispectral WorldView-2 imagery from top of atmosphere sensor radiance (LTOA) to surface reflectance (Ps) values.

The empirical line method has been used to convert at-sensor radiance values to surface reflectance for numerous multispectral satellites (Clark & Pellikka 2005; Hadjimitsis et al. 2009; Karpouzli & Malthus 2003), and airborne hyperspectral sensors (Smith & Milton 1999). It is based on establishing a relationship between LTOA values and Ps values measured from calibration targets located within the image area. The Ps values of the calibration targets are measured using field spectrometers and ideally should cover the range of albedo values found within the imagery. The LTOA values are then extracted from the imagery and compared with the field measured Ps values to define prediction equations to convert image derived LTOA to Ps values for each waveband (Smith & Milton 1999).

The relationship between radiance and reflectance across the whole data range (0-100%) is quadratic (Moran et al. 1990). However, correction of imagery using empirical line methods typically based on a linear relationship. This is due to the fact that the relationship between radiance and reflectance between 0-65% has been found to be essentially linear, allowing interpolation with minimal error (Clark & Pellikka 2005; Moran et al, 1990).

It must be noted that calibration of imagery using the empirical line method involves the simplification of a number of significant factors (Hadjimitsis et al. 2009). The assumptions are that both atmospheric conditions and illumination intensity are uniform across the image and that the image consists of features all with lambertian reflectance properties (Smith & Milton 1999). The degree of deviation from these assumptions is an important factor affecting the accuracy of the prediction equations developed. Karpouzli & Malthus (2003) used empirical line methods to atmospherically correct IKONOS satellite data using nine pseudo invariant targets (PIFs) and reported highly satisfactory results. They highlighted the fact that the increased spatial resolution of the IKONOS sensor enabled a large number of targets to be identified, and suggested that increasing the number of calibration targets may contribute to the reduction of error between image and field measured Ps.

Three calibration panels and seven pseudo invariant features (PIFs) were used in this current work as calibration targets to define non-linear equations for each of the eight WorldView-2 multispectral bands. A further 10 validation targets were then used to assess the reliability of the prediction equations derived for each waveband.

2. METHODS

2.1 Study Area & Data

One of the major fields of spring wheat in Iran is located in Golestan Province. The study was conducted during spring season in 2017 (37º 26' N, 55º 19' E). The field size was 1.8×1.5 km^2. The soil texture in this area varies between sand and limestone.

The WorldView-2 satellite consists of one panchromatic band (450-800 nm) with a spatial resolution of 0.5 m (resampled from 0.46m) and eight multispectral bands; Coastal (400-450 nm), Blue (450-510 nm), Green (510-580 nm), Yellow (585- 625 nm), Red (630-690 nm), Red Edge (705-745 nm), NIR 1 (770-895 nm) and NIR 2 (860-1040 nm) with a spectral resolution of 2.0 m resampled from 1.84 m.

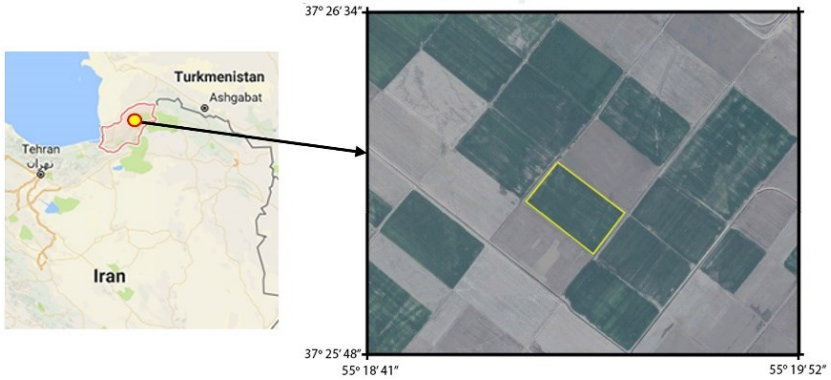

Figure 1. Location of study area.

2.2 Image pre-processing

Orthorectification of the imagery was undertaken using the sensor's Rational Polynomial Coefficients (RPC) and ground control points. A one second Shuttle RADAR Topography Mission (SRTM) Digital Elevation Model (DEM) version 1 obtained from Geoscience Australia was used in the orthorectification process. Coordinates for 30 ground control points (GCPs) distributed evenly across the imagery were acquired using a dGPS (overall average positional accuracy for the X and Y coordinates was 8.9 mm). The RPC files are supplied with the imagery. Eight GCPs were used in the orthorectification of Image 2 while ten GCPs were used for Image 1 The overall accuracy assessment of the orthorectification based on six independent GCPs resulted in an average Root Mean Square Error (RMSE) of 1.7 m. To account for sensor characteristics, the images were converted from DN to *LTOA* spectral radiance using Eq. 1:

$$L_{\lambda Pixel,band} = \frac{K_{Band} * Q_{Pixel,Band}}{\Delta_{\lambda Band}} \quad (1)$$

Where: $L_{\lambda Pixel,band}$ represents TOA spectral radiance image pixels (W-m^{-2}-sr^{-1}-µm^{-1}); K_{Band} is the absolute radiometric calibration factor (W-m^{-2}-sr^{-1}-count^{-1}) for a given band; $Q_{Pixel,Band}$ represents the radiometrically corrected image pixels (DN); and $\Delta_{\lambda Band}$ is the effective bandwidth (µm) for a given band. The absolute calibration (K_{Band}) and effective bandwidth ($\Delta_{\lambda Band}$) parameters for each band are obtained from the metadata supplied with the imagery.

2.3 Field spectra.

This study utilised a combination of both calibration panels and PIFs to convert *LTOA* values to *Ps*. Smith & Milton (1999) and Karpouzli & Malthus (2003) suggest that PIF targets used for empirical line correction should have the following characteristics: be spectrally homogenous; near lambertian and horizontal; devoid of vegetation; cover an area greater than three times the pixel size of the sensor; and cover a range of reflectance values. For this work a total of 20 PIFs were measured in the field along with three calibration panels.

Spectra were captured using a 25º field of view (FoV) at nadir with the averaging sample spectrum set to 25. The sensor height was set to 1 m for targets on land and 0.5 m over water, resulting in a ground view of ~44 cm and ~22 cm in diameter, respectively. A minimum of one and maximum of four spectral samples were collected between each white reference. The number of samples obtained for each target was dependent on the variance observed within the target, with between 8 and 20 samples collected per target.

The area sub-sampled for most targets was 24 m^2. However, larger areas were sampled for targets such as synthetic bowlinggreen, golf green, rock outcrop and bitumen road, as these targets could be easily identified within the imagery. The location of each target was recorded using a hand-held GPS with an accuracy of ±3m. The majority of targets, with the exception of the open water targets from Jabiluka billabong, were located within Image 2. The only target located within the overlap of the two images was the rock outcrop (V15 in Table 2).

The three types of calibration panels used in this project were selected as together they spanned a wide range of reflectance values. Previous laboratory spectral measurements had also shown they would be suitable targets for use as calibration panels (Pfitzner et al. 2010). The panels were laid out on the Jabiru sports field, on the morning of the satellite overpass, and spectra were collected immediately after the satellite overpass. Targets used for the prediction

equation were selected based on the fact that they represented a range of reflectance values (dark to bright values), were spectrally homogenous (summarised by mean CoV) and were likely to be invariant features. The one vegetation target used for the prediction equation was captured on the day of the image acquisition.

2.4 Empirical line calibration

The averaged field spectra (P_s) were re-sampled to the relative spectral response of each WorldView-2 waveband using the spectral re-sampling tool in ENVI 4.7 ITT Visual Information Solutions. The average *LTOA* values associated with each calibration panel and PIF were then extracted from the imagery. A non-linear quadratic relationship Eq. (2) was fitted between *LTOA* and *Ps* using the statistical software Statistica 6.1c Stat Soft, Inc:

$$y = a_1 + b_1 x + b_2 x^2 \quad (2)$$

where y is the response representing P_s, x is the predictor representing LTOA, a is the intercept, and b_1 and b_2 are the fitting coefficients. The intercept (a) represents the additive effect due to atmospheric path radiance and the slope parameters (b_1, b_2) represent the correction for atmospheric attenuation (Hadjimitsis et al. 2009; Karpouzli & Malthus 2003).

3. RESULTS & DISCUSSION

3.1 Predication equations

The combination of calibration panels and PIF targets enabled the development of a non-linear relationship between *LTOA* and *P*s. A total of ten targets were used to derive the prediction equation, resulting in statistically significant relationships for each waveband ($R^2 = 0.98$, $P < 0.0001$, 97.5% confidence level). In common with previous studies using empirical line methods (Clark & Pellikka 2005; Karpouzli, & Malthus 2003) the correction needed for atmospheric path radiance (represented by the intercept of the x axis) was greatest in the shorter wavelengths and decreased as wavelength increased.

3.2 Validation targets.

Summary statistics for each band are presented in Table 1. The overall RMSE values for each band show that there was a high degree of agreement between the satellite derived *Ps* values and field measured *P*s values for the 10 validation targets. Six of the eight bands recorded RMSE values below 2% with the coastal band recording the lowest value (0.54%). The red-edge and two NIR bands recorded the highest RMSE values. The increased error in the NIR bands can be attributed to the prediction equations, which produced negative reflectance values at very low *LTOA* values.

Table 1. Summary statistics derived from the validation targets for each waveband.

Band	RMSE (%)
1	0.54
2	1.1
3	1.3
4	1.7
5	1.5
6	2.3
7	1.9
8	2.2

The WorldView-2 spectral signatures predicted for V15 (rock outcrop) from the two different off nadir view angles are presented in figure 2. The RMSE values (Image 1 = 0.63, Image 2 = 0.98) and MAPE values (Image 1 = 2.5, Image 2 = 4.1) for each image and the spectral signatures demonstrate that the prediction equations were able to account for the different view angles with very little difference in the predicted *Ps* values for each image.

4. CONCLUSION

The combination of both calibration panels and PIF targets enabled the development of prediction equations covering the full range of albedo values within the image. Assessment of the prediction equations based on 17 independent validation targets show that overall accuracy was high, with RMSE values between 0.54% and 2.3% across the eight multispectral bands. The results of this study show that the empirical line method using non-linear prediction equations can be used to successfully calibrate the eight multispectral bands of the WorldView-2 satellite image to surface reflectance.

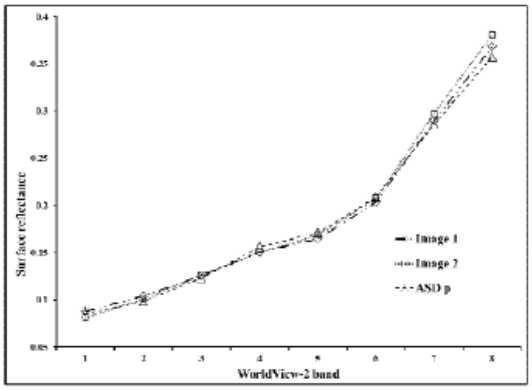

Figure 2. Comparison of the WorldView-2 spectral signature for the validation target (Rock outcrop), Image 1 and Image 2 are the predicted *P*s values derived from different view angles and the ASD p is the field measured *P*s.

REFERENCES

P. S. Chavez, Jr. "Image Based Atmospheric Corrections – Revisited and Improved," Photogrammetric Engineering and Remote Sensing, vol. 62, p.p. 1025-1036, 1996.

B. Clark P. Pellikka "The Development of a Land Use Change Detection Methodology for Mapping the Taita Hills, South-East Kenya: Radiometric Corrections." Proceedings of the 31st International Symposium on Remote Sensing of Environment (ISRSE), 20-24 June, St Petersburg, Russian Federation. CDPublication, no page numbers. 2005

D. Hadjimitsis, C. Clayton, A. Retalis. "The use of selected pseudo-invariant targets for the application of atmospheric correction in multi-temporal studies using satellite remotely sensed imagery" International Journal of Applied Earth Observation and Geoinformation vol 11, p.p. 192-200, 2009.

E. Karpouzli, T. Malthus, "The empirical line method for the atmospheric correction of IKONOS imagery," International Journal of Remote Sensing, vol. 24, p.p. 1143-1150, 2003.

M. S. Moran, R. D. Jackson, G. F. Hart, P. N. Slater, R.J. Bartell, S.F. Biggar, D.I. Gellman, R.P. Santer, "Obtaining Surface Reflectance Factors from Atmospheric and View Angle Corrected SPOT1 HRV Data," Remote Sensing of Environment, vol 32, p.p. 203-214, 1990.

K. Pfitzner, G. Staben, R. Bartolo, "The Spectral Reflectance of Common Artificial Pseudo Invariant Materials" Proceedings of the 15th Australasian Remote Sensing & Photogrammetry Conference (ARSPC) 13-17 September, Alice Springs, Australia. 2010.

G. M. Smith, E. J. Milton, "The use of the empirical line method to calibrate remotely sensed data," International Journal of Remote Sensing, vol. 20, 2635-2662, 1999.

S. M. Vicente-Serrano, F. Perez-Cabello, T. Lasanta "Assessment of radiometric correction techniques in analysing vegetation variability and change using time series of Landsat images" Remote Sensing of Environment vol. 112, p.p. 3916– 3934, 2008.